

Characteristics of the Tether Line for Airborne Vehicles at Sea

STUART G. GATHMAN

*Atmospheric Physics Branch
Ocean Sciences Division*

September 30, 1975



NAVAL RESEARCH LABORATORY
Washington, D.C.

Approved for public release; distribution unlimited.

(continued from block 20)

layer between the vehicle and the surface from surface measurements alone if the vehicle can be seen; determining the mean wind in the layer between the vehicle and the surface if the vehicle can not be seen but with the additional knowledge of the vehicle altitude; calculating the flight path of the tethered vehicle as it leaves the flight deck to minimize the probability of diving to the surface in the turbulent eddies downwind of the ship; and calculating the maximum altitude which can be obtained, taking into account the force of the wind on the tether line.

CONTENTS

INTRODUCTION	1
PART I — PRELIMINARY PREDICTION OF KITE BALLOON FLIGHT PATH	1
PART II — MECHANICS OF KITE BALLOON FLIGHT	4
SHIPBOARD KYTOON OPERATION	18
REFERENCES	23
APPENDIX A — Program to Determine Altitude and Line of Sight Angle of a Tethered Vehicle	24

CHARACTERISTICS OF THE TETHER LINE FOR AIRBORNE VEHICLES AT SEA

INTRODUCTION

The study of fogs and other boundary layer phenomena over the sea requires an economical platform on which to locate sensing instruments. Practically speaking, we are limited at sea to tower heights of perhaps 100 ft (these being the masts of ships). Free-flight balloons, sounding rockets, and dropsondes, as well as manned aircraft, penetrate the area of interest. These, however, tend to be expensive in studies which require many hours of measurements. The small tethered kite balloon or parafoil can provide an economical answer to sounding, to averaging meteorological parameters in the boundary layer, and to collecting samples of fog droplets.

The altitude of the kite balloon is an extremely important factor which must be accurately known in order that the other data being measured will have meaning. Historically, many approaches have been used. An ordinary radiosonde baroswitch is not particularly useful in this application because the altitude of the kite balloon is not necessarily a monotonically decreasing or increasing function of time, as it is in the ordinary free-flight balloon or dropsonde. Triangulation by observers at the ground has been used successfully. Another approach is to calculate the geometry of the tether catenary, using measurable single-point parameters at the ground. Other forms of mechanical pressure gauges obviously exist, but most are too heavy to be useful in the small kite balloon system.

With the recent availability of accurate solid state pressure gauges in the form of integrated circuits, the altitude of the kite balloon can now be continuously monitored. Thus, probing the boundary layer with a tethered vehicle becomes attractive.

PART I — PRELIMINARY PREDICTION OF KITE BALLOON FLIGHT PATH

A kite balloon is different from both the kite and the spherical balloon in that the lift it experiences is the result of both static and aerodynamic forces. Consider the diagram in Fig. 1 in which the kite balloon is flying at its maximum altitude h above the ground surface. If the angle of the tether line with respect to the horizontal is zero at the ground, the tethered vehicle is at its maximum altitude. This is a special case which lends itself to a simple analytic solution which, although it neglects the wind drag on the tether line, nevertheless predicts with certain limitations the maximum altitude which a tethered vehicle can obtain, given the lift and drag of the vehicle as functions of the windspeed. The maximum altitude is an important parameter in boundary-layer sounding (an adjustment in instrumentation load may be necessary to obtain a desired altitude). The following analysis is intended to be used only as a rough preflight maximum-altitude predictor. A more accurate analysis incorporating the wind loading on the line is presented in Part II of this

report. If the effect of wind drag on the line is neglected, the tether line forms a catenary which can be described in the x,y coordinate system by the equation

$$y = c [\cosh (x/c)]$$

where c is the catenary parameter. The catenary has the property that the line tension is everywhere equal to the unit gravitational force w on the cable times the distance of the point on the cable above the x axis in Fig. 1. Thus at the vertex, point $(c, 0)$, the tension T_v is horizontal and has the value

$$T_v = cw. \quad (1)$$

At the kite balloon the magnitude of the tension T_k is

$$T_k = (c + h)w. \quad (2)$$

The vertical component of this tension is produced by the weight of the cable and is given as

$$T_k \sin \theta = sw, \quad (3)$$

where s is the length of the cable. The horizontal component is the same as T_v ;

$$T_k \cos \theta = T_v = cw. \quad (4)$$

Then from Eqs. (2), (3), and (4)

$$\sin \theta = s/(c + h)$$

$$1 - \cos \theta = h/(c + h)$$

and, therefore,

$$\tan \theta/2 = h/s. \quad (5)$$

If the forces acting on the kite balloon are equated, the vertical lift L is balanced by the total gravitational force on the cable ws , and the instrument payload. The horizontal component of the tension in the tether line at the kite balloon is balanced by the drag forces D on the kite balloon. These relationships may be expressed as

$$T_k \sin \theta = L - I$$

$$T_k \cos \theta = D$$

or

$$\tan \theta = (L - I)/D$$

From Eqs. (5) and (3), we have

$$h = \frac{(L - I)}{w} \tan \left\{ \frac{\arctan}{2} [(L - I)/D] \right\}. \quad (6)$$

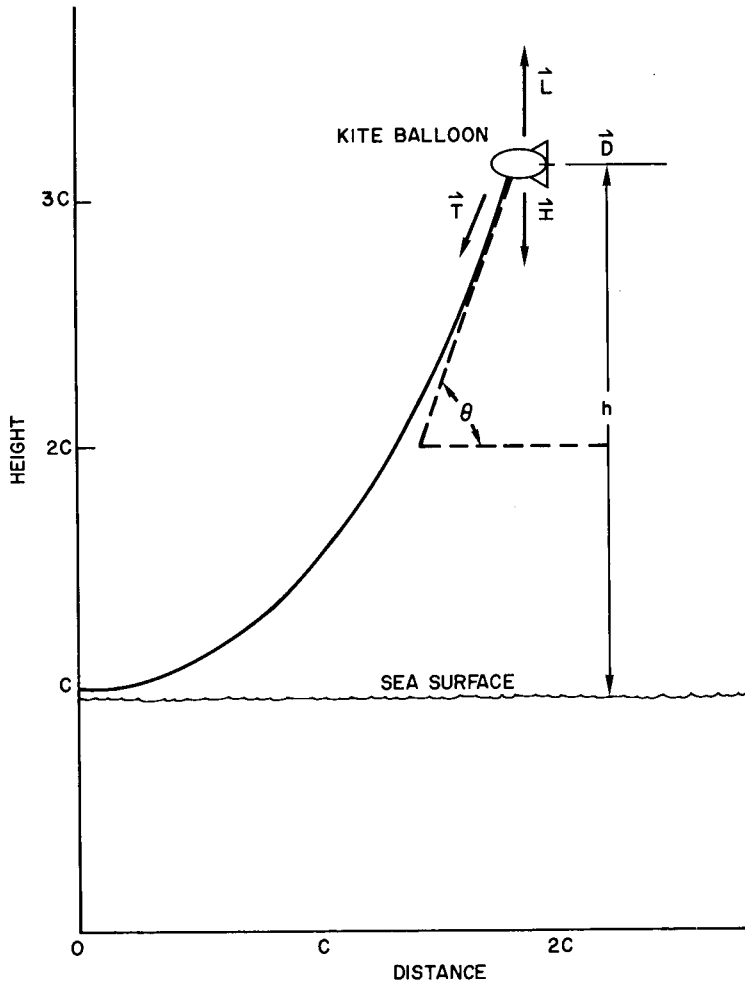


Fig. 1 — Forces acting on a kite balloon flying at maximum altitude h above the sea surface at the end of a tether line

The equations for lift and drag forces on an airfoil in an airstream of relative velocity V are given by

$$L' = C_l A \rho V^2 / 2$$

$$D = C_d A \rho V^2 / 2$$

where C_l and C_d are dimensionless lift and drag coefficients, ρ the density of air, and A the area of the projection of the airfoil on the plane of the chord. The lift equation for the kite balloon has the added buoyancy term B and may be expressed as

$$L = C_l A \rho V^2 / 2 + B. \tag{7}$$

The drag force can then be expressed in terms of lift as

$$D = (L - B)C_d/C_l. \quad (8)$$

The lift L can be measured experimentally or is given by the manufacturer for the specific kite balloon. An expression for the maximum height h to which the kite balloon will rise can be given if the observables of lift payload, buoyancy, unit gravitational forces on the cable, and the ratio of C_l to C_d are known:

$$h = \frac{(L - I)}{w} \tan \frac{\arctan}{2} [(C_l/C_d) (L - I)/(L - B)] . \quad (9)$$

Equation (7) simplifies the actual lift because the kite balloon changes altitude with respect to the horizontal as the relative wind increases from calm to moderate. In a calm, the kite balloon may stand almost vertically with the nose pointing upward. As the wind increases, the angle of attack changes to that fixed by the bridle ropes.

Figure 2 shows plots of the maximum altitudes predicted from Eq. (9) for a realistic range of windspeeds for various ratios of the lift coefficient to that of the drag coefficient. These curves show the great advantage provided by the aerodynamically shaped kite balloon, with the value of C_l/C_d above 0.6 when it is compared with a tethered spherical balloon with its value of C_l/C_d less than 0.1. In winds greater than about 2.5 m/sec the spherical balloons are pulled by the wind drag almost to the earth's surface. When the windspeed is above 5 m/sec, the kite balloon ceases to act like a balloon and becomes a kite. It is then capable of heavier-than-air flight.

The effect of wind drag on the tether line has been neglected in the previous analysis. A more accurate model will take into account both the effect of wind on the vehicle and on the tether line.

PART II — MECHANICS OF KITE BALLOON FLIGHT

Partial analytical solutions to the problem of wind drag on a tether line have been published by Willers [1] and by Kochin [2]. Digital integration techniques now make it easy to take into account all of the pertinent parameters to model the actual flight characteristics of particular vehicles.

Consider now an element of line shown in Fig. 3. The length of this element is ds . The tension at the lower end of the element will be denoted by vector T_1 and that at the upper end by vector T_2 . These vectors differ from each other by a small amount dT . The difference vector can be broken down into a component parallel with T_1 and a component perpendicular to it. The parallel component can be represented to the first approximation by the difference in the magnitude of the tensions between the two points, whereas the perpendicular component is represented by the $|T_1| d\theta$, where $d\theta$ is the included angle between T_1 and T_2 .

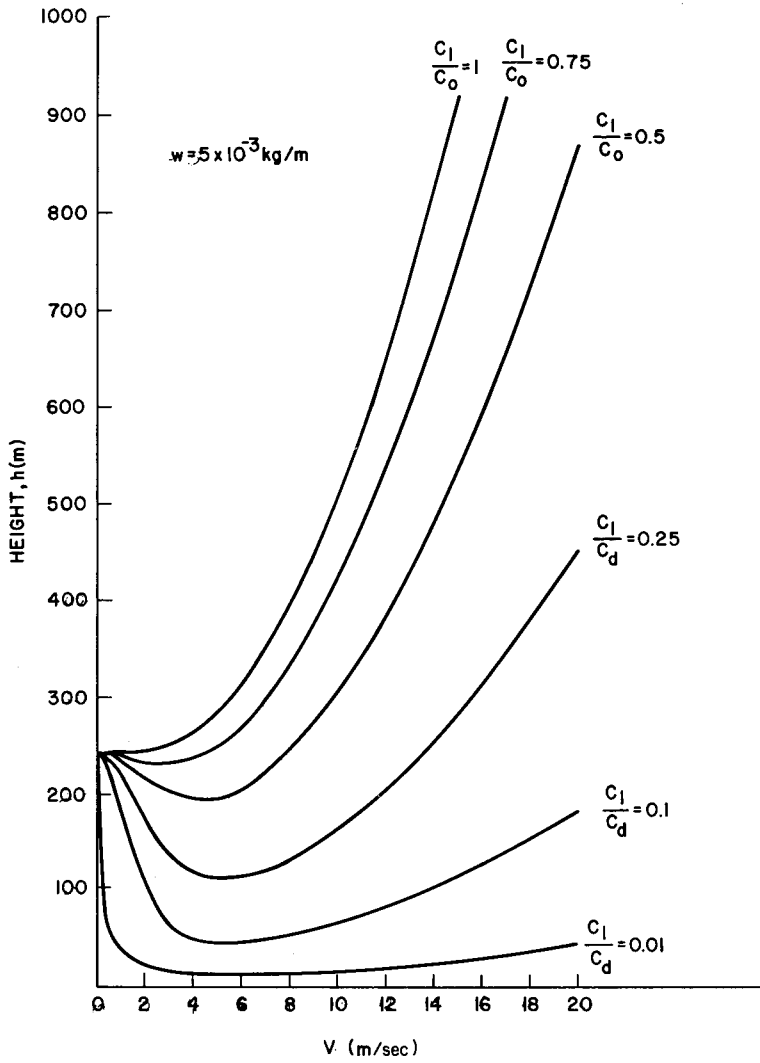


Fig. 2 — Plot of the maximum altitudes obtainable for a kite balloon as a function of windspeed. The unit gravitational force on the line is 0.049 N/m. The lift constants of Eq. (7) for this calculation are $B = 11.76 \text{ N}$ and $C_{\ell} A \rho / 2 = 0.39 \text{ N sec}^2 / \text{m}^2$.

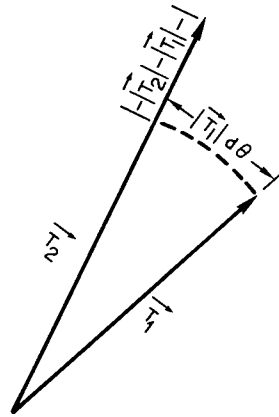
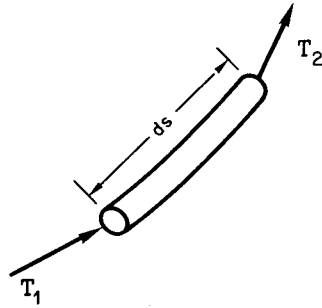


Fig. 3 — Vectors of tensions acting on an infinitesimal piece of tether line

Willers [1] and Kochin [2] made the assumption that the force of the wind on the line is only in a direction perpendicular to the line, whereas the force of gravity affects both the components. Therefore, if the forces in the parallel direction are balanced,

$$dT = w ds \sin \theta.$$

In the perpendicular direction,

$$T d\theta = w ds \cos \theta + F_n ds$$

where F_n is the force of the wind normal to the line and may be expressed by

$$F_n = k v_n^2.$$

Now $v_n = v_w \sin \theta$, where v_w is the wind velocity in the horizontal direction. Therefore,

$$F_n = kv_w^2 \sin^2 \theta,$$

and Eq (3) may be written as

$$Td\theta = w ds \cos \theta + kv_w^2 \sin^2 \theta ds.$$

Note also that the Cartesian coordinates are related to s and θ by the following differential equations;

$$dx/ds = \cos \theta$$

$$dy/ds = \sin \theta.$$

Hence we have a system of four simultaneous first-order differential equations which describe the tether line:

$$\frac{dT}{ds} = w \sin \theta$$

$$\frac{d\theta}{ds} = (w \cos \theta + F \sin^2 \theta)/T$$

$$\frac{dx}{ds} = \cos \theta \tag{10}$$

$$\frac{dy}{ds} = \sin \theta,$$

where F is the horizontal wind drag force per unit cable length and w is the gravitation force per unit length. These two parameters describe the physical forces attributable to the line. They are expressed as

$$F = \frac{1.1 \rho d}{2} v_w^2 \tag{11}$$

and

$$w = g \frac{\pi}{4} d^2 \mu,$$

where ρ is the density of the air, d is the area of the line per unit length presented to the component of the wind normal to the line (or simply the diameter of the line times 1 m), g is the acceleration of gravity, and μ the density of the line material.

Given the initial values of T , θ , x , y at $s = 0$ and the above differential equations, the values at different values of s can easily be computed by finite difference techniques. Consider Table 1. (A simple, basic program for this purpose is given in Appendix A.)

Table 1

$T_0,$	$\theta_0,$	$x_0,$	$y_0,$	s_0
$T_1,$	$\theta_1,$	$x_1,$	$y_1,$	s_1
$T_2,$	$\theta_2,$	$x_2,$	$y_2,$	s_2
...
...
$T_n,$	$\theta_n,$	$x_n,$	$y_n,$	s_n

Values in adjacent rows differ from each other by only small amounts of line length which can be made as small as necessary for the accuracy required.

Here, T_0 is the tension measured at the ground and θ_0 is the angle measured at the ground. The length of line deployed is known by direct measurement; if the mean wind-speed and the diameter of the line as well as its density are known, and if the coordinate system is set such that x_0, y_0 is the point (0,0), then the integration process can be continued until s_n equals s . At this time, the altitude y_n can be read from the computer printout. It is not necessary to see the vehicle, but if accurate measurements of tension and the departure angle as well as the metered reading of length of line are available as well as an estimate of wind, then the altitude is known. The problem of measuring the tension and departure angle on a moving ship, however, makes this method less desirable than using a pressure altimeter. This method can be used to obtain also an equivalent wind value throughout the altitude occupied by the tether lines.

If the vehicle can be sighted, then the angle α which the line of sight makes with the horizontal can be calculated as the arctan (y_n/x_n). With a digital computer, integration can start with the initial conditions of T_0 and θ_0 and continue to $s_n = s$. At this point, the measured angle and that calculated by the program can be compared. If they are not equal, new values of wind can be tried until the appropriate wind is found. Thus from ground-based measurements alone, both the equivalent windspeed and the height of the vehicle can be calculated.

If the vehicle cannot be seen (as in fog for example), and if the altitude is measured by an onboard pressure altimeter, then given the same initial surface conditions of T_0 , θ_0 , and the length of line, the digital computer can try various values of windspeed to determine which gives the best agreement between the measured altitude and the calculated altitude. An illustrative sample is given below.

A graphical technique was developed by the late Horace M. Trent, in an unpublished communication, whereby with known measurements of tension and departure angle at the ground, the length of the line, the density of the line, and its diameter with either the angle α or an independent altitude determination, the mean wind can be calculated. This method involves the set of curves which represents analog solutions to the set of simultaneous differential equations shown in Eq. (10) as rectangular plots of s and h . In Figs. 4 through 11, each curve plotted represents a solution of this system for a given set of values of the parameters ws/T_0 and Fs/T_0 and given values for the initial conditions of tension and departure angle at the ground. The initial values of x_0/s and y_0/s were taken to be zero. From each curve thus obtained, h/s was read and plotted as a function of $(\alpha - \theta_0)$, where α is the arctan (h/x).

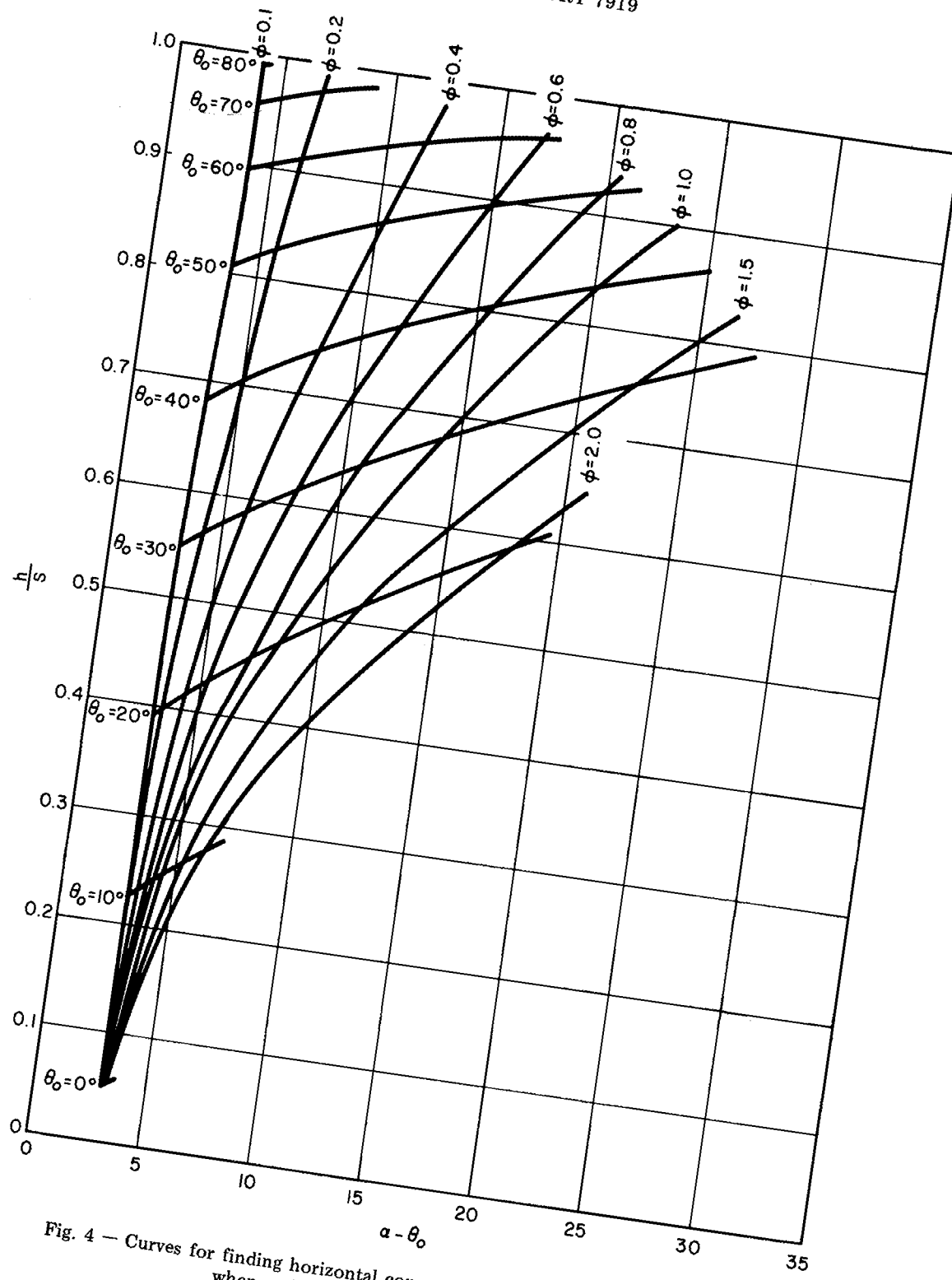


Fig. 4 - Curves for finding horizontal component of wind drag on cable when $ws/T_0 = 0.1$ and $\varphi = Fs/T_0$

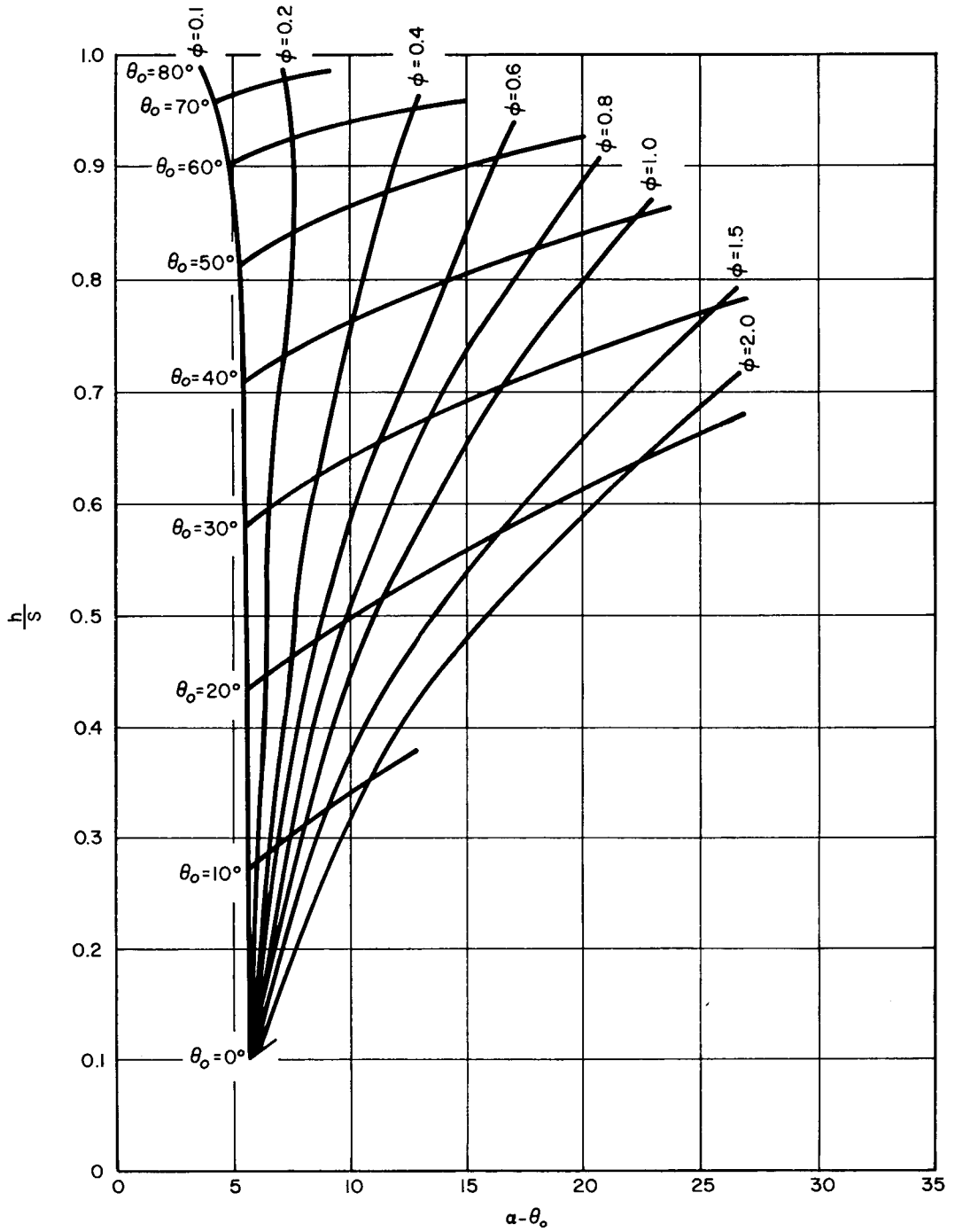


Fig. 5 — Curves for finding horizontal component of wind drag on cable when $ws/T_0 = 0.2$ and $\phi = Fs/T_0$

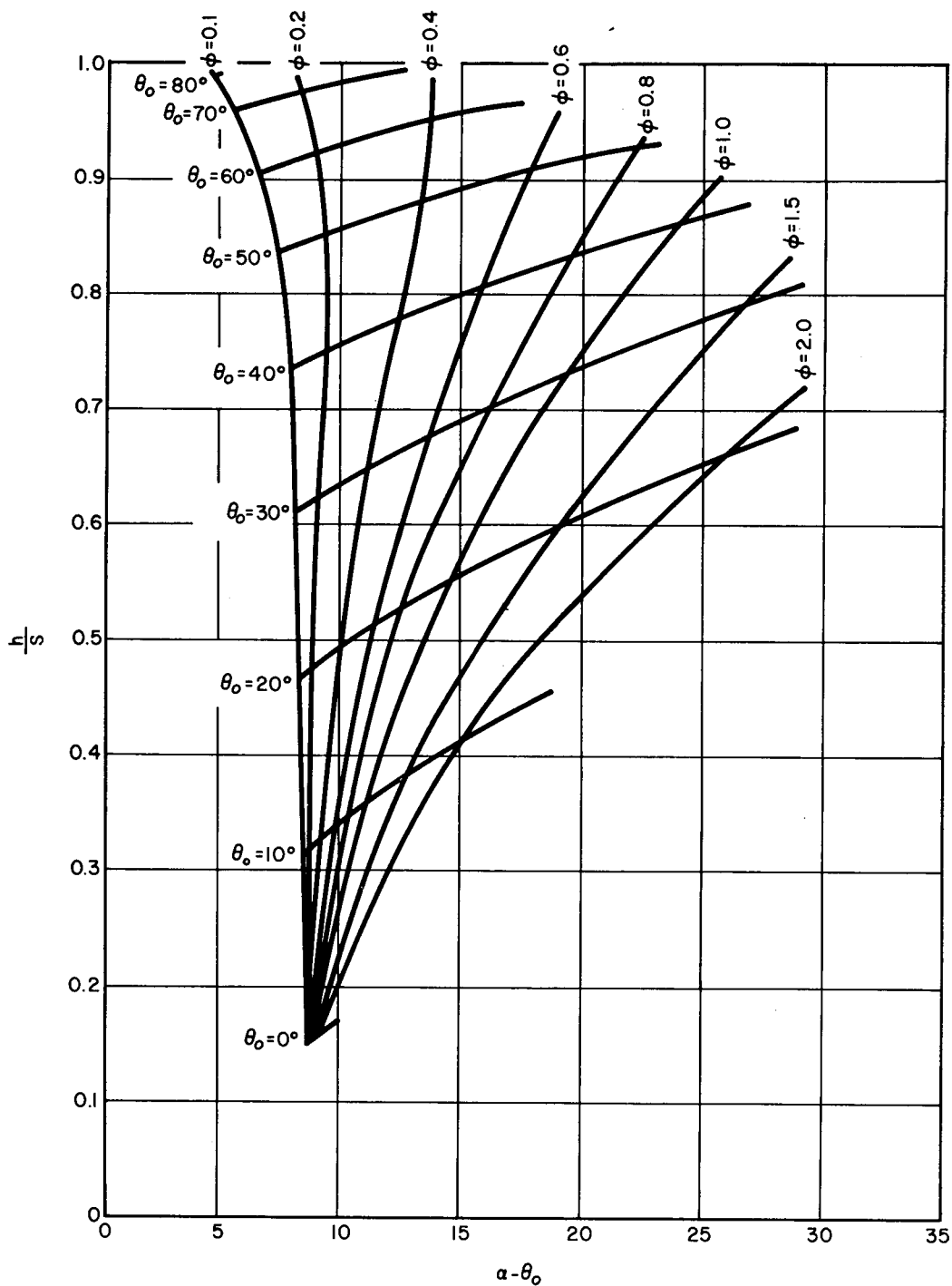


Fig. 6 — Curves for finding horizontal component of wind drag on cable when $ws/T_0 = 0.3$ and $\phi = Fs/T_0$

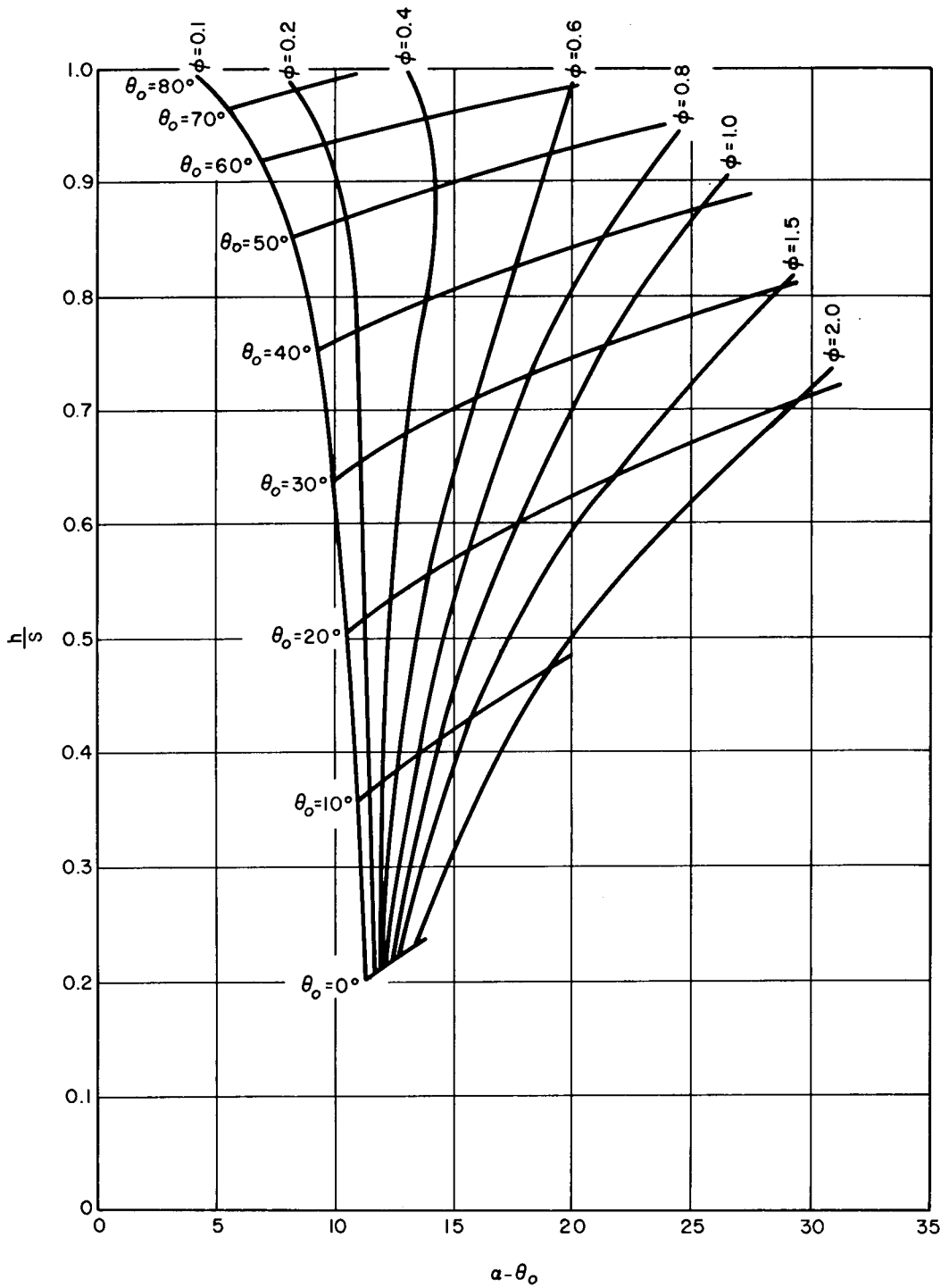


Fig. 7 — Curves for finding horizontal component of wind drag on cable when $ws/T_0 = 0.4$ and $\phi = F_s/T_0$

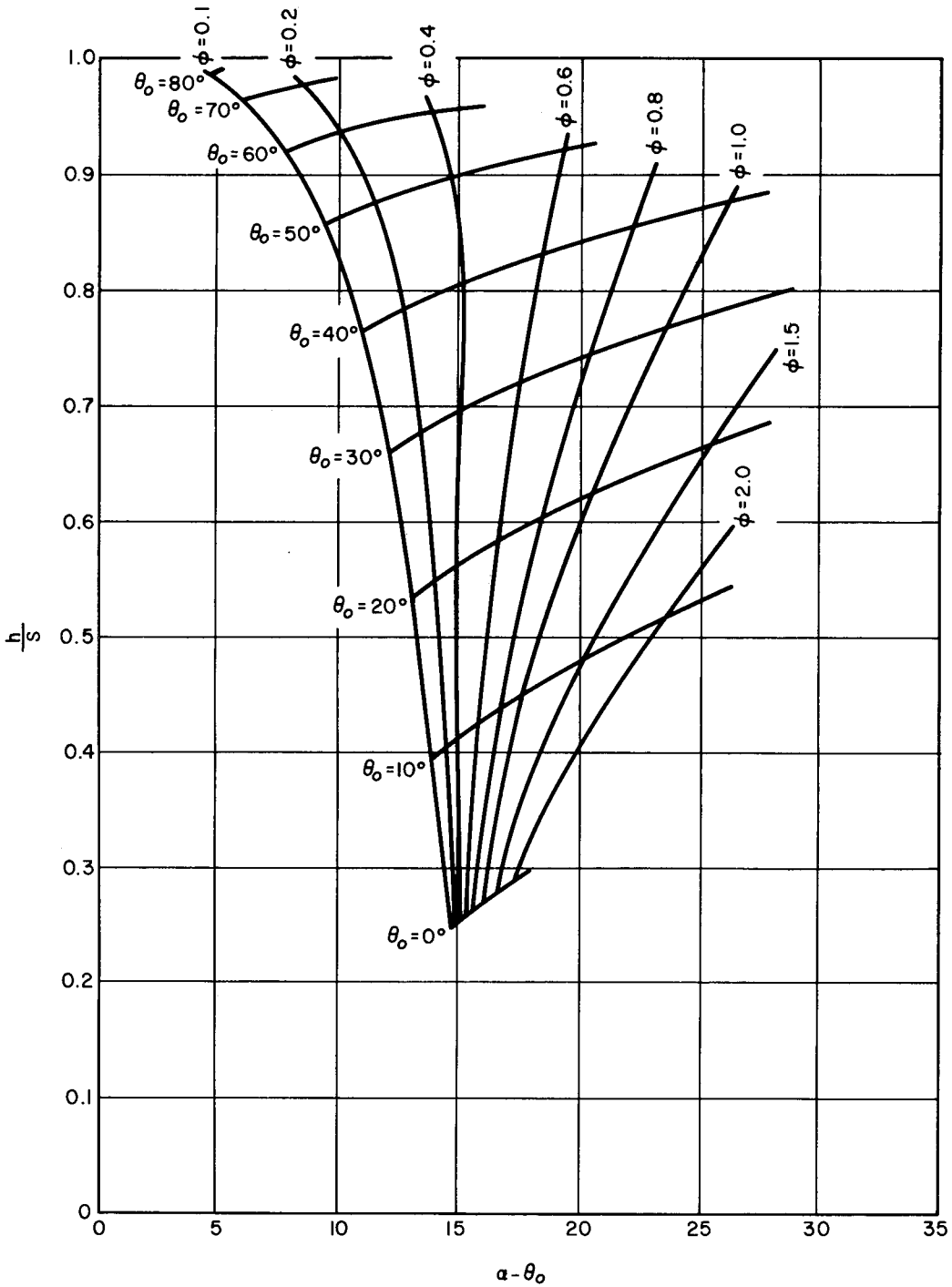


Fig. 8 — Curves for finding horizontal component of wind drag on cable when $ws/T_0 = 0.5$ and $\varphi = Fs/T_0$

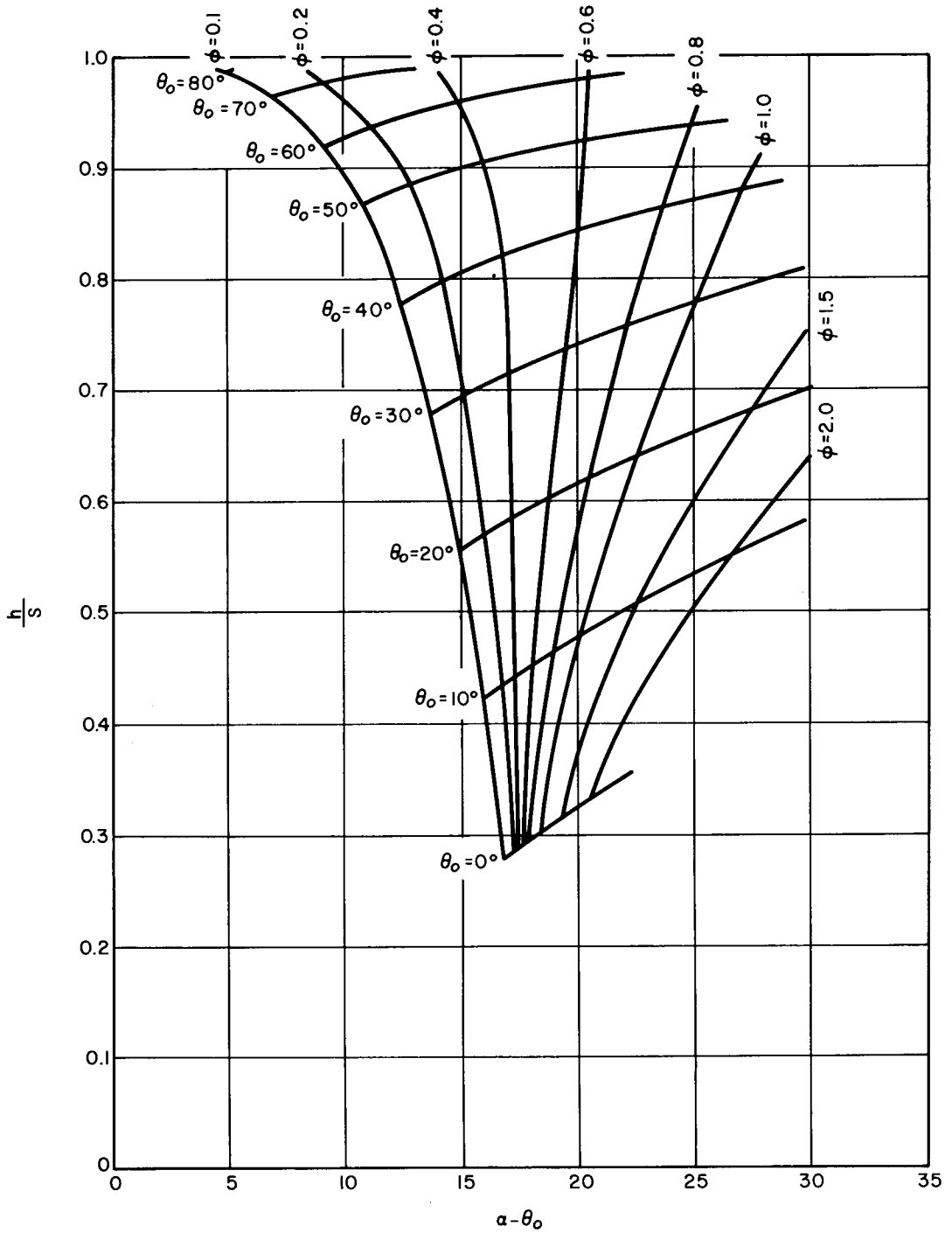


Fig. 9 — Curves for finding horizontal component of wind drag on cable when $ws/T_0 = 0.6$ and $\phi = Fs/T_0$

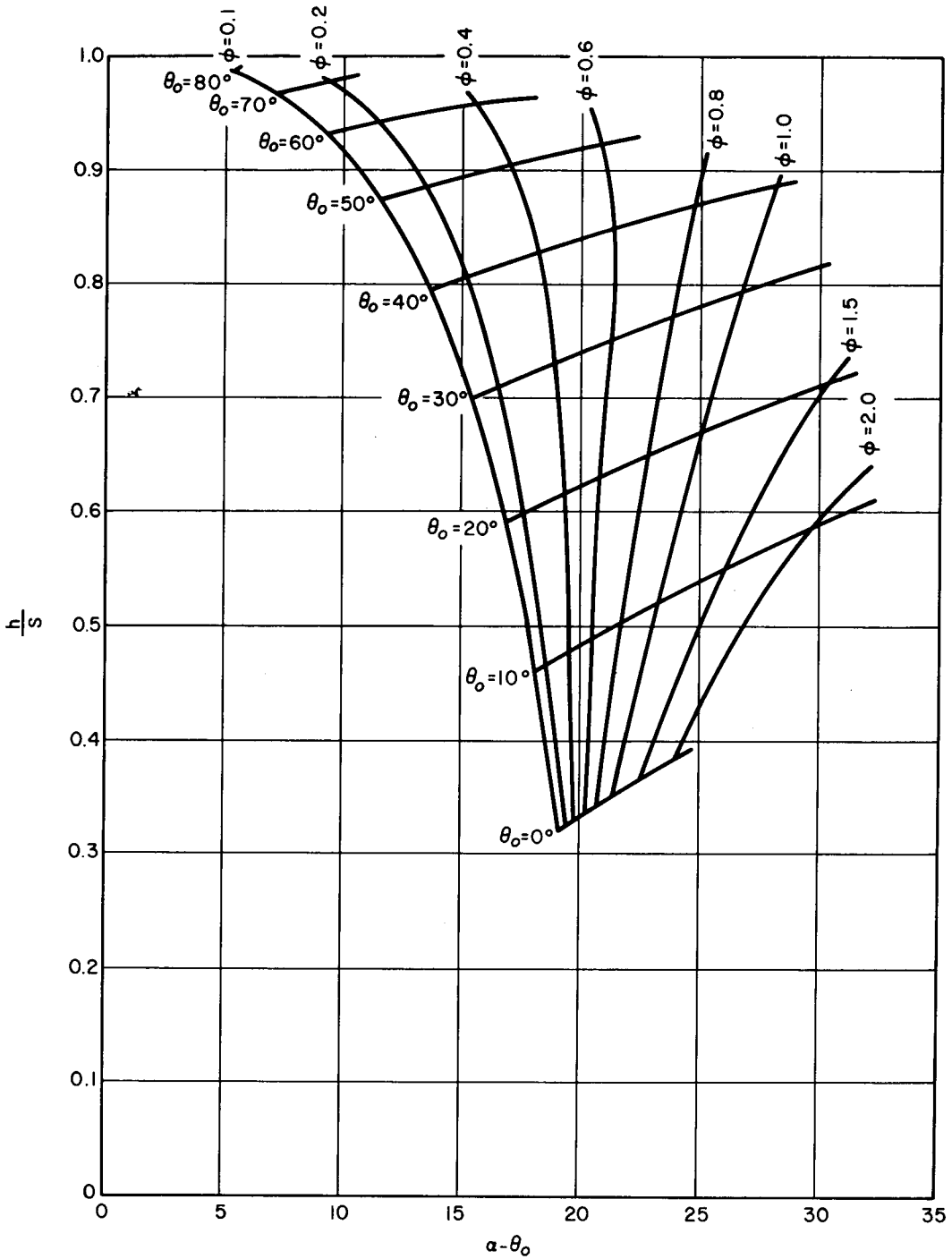


Fig. 10 — Curves for finding horizontal component of wind drag on cable when $ws/T_0 = 0.7$ and $\phi = Fs/T_0$

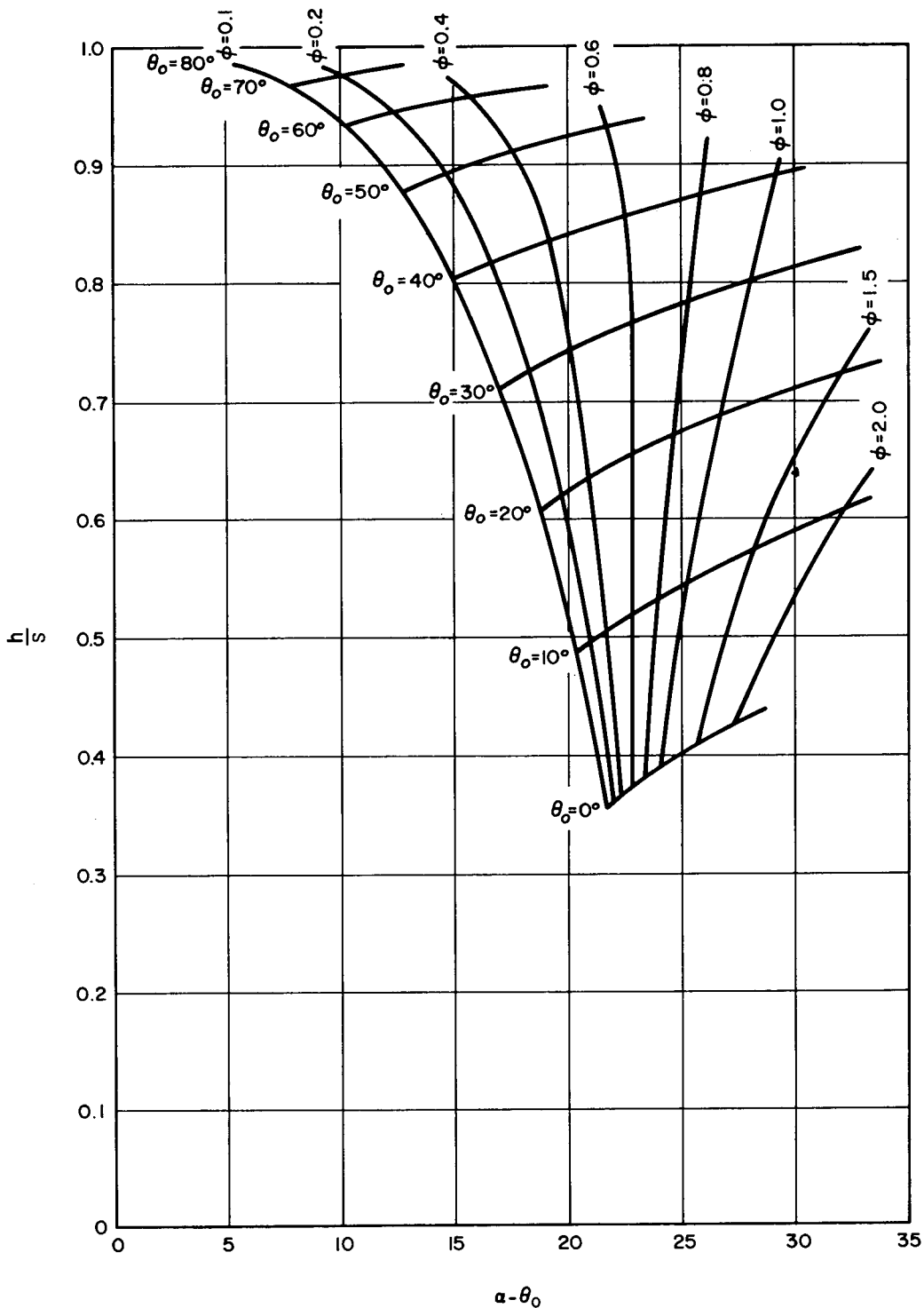


Fig. 11 — Curves for finding horizontal component of wind drag on cable when $ws/T_0 = 0.8$ and $\phi = Fs/T_0$

This set of curves has two uses. First of all, if the vehicle can be seen, the elevation angle α between the line of sight and the horizontal, and the angle θ_0 can both be measured, and the ratio of h/s can be read directly from one of these curves. If the length of line is known, the altitude is obtained approximately. Given the gravitational force on a unit length of line, the measured tension, and either $\alpha - \theta_0$ and θ_0 or h and θ_0 , the curve most applicable to the situation is known, and φ , which is a function of the force F acting on the line, can be found. This in turn is directly related to the equivalent windspeed if the diameter of the line is known.

As an illustrative example showing both the graphical method and the program in Appendix A (designed to obtain the effective windspeed for a layer of air through which the balloon cable is suspended), consider the following observations:

Gravitational force on unit length of cable	$w = 0.01156 \text{ N/m}$
Lengths of cable	$s = 500 \text{ m}$
Elevation angle of balloon	$\alpha = 63^\circ$
Departure angle of cable	$\theta = 46.6^\circ$
Tension at the reel	$T_0 = 46.55 \text{ n}$
Diameter of cable	$d = 0.001 \text{ m.}$

In the graphical method, first compute (ws/T_0) to find the appropriate figure to use:

$$\frac{ws}{T_0} = \frac{0.01156 \times 500}{46.55} = 0.12 .$$

This value is closest to $(ws/T_0) = 0.1$ used in the solutions on Fig. 4. The point where $\alpha - \theta_0 = 16.4^\circ$ and $\theta_0 = 46.6^\circ$ indicates that $\varphi = 0.73$ and $h/s = 0.86$. Therefore the wind drag per unit length is

$$F = \frac{\varphi T_0}{s} = 0.0679 \text{ N,}$$

and

$$h = 430 \text{ m.}$$

From Eq. (11), with the density of air being 1.3 kg/m^3 ,

$$v_w = \sqrt{\frac{2F}{1.1 \rho d}} = \sqrt{\frac{2 (0.0679)}{(1.1) (1.3) (0.001)}} = 9.7 \text{ m/sec.}$$

Figure 12 is the example (using the program in Appendix A) where the interchange between a keyboard terminal and a time-sharing computer is reproduced. The data requested by the computer are underlined. In this particular case, the same input information was entered into the digital computer as was used in the graphical analysis above. The results show that the graphical and digital methods agree to within 3%. This is the kind of accuracy expected from the use of graphical methods.

STUART G. GATHMAN

WHAT IS LENGTH OF ROPE IN METERS ?500
WHAT IS DIAMETER OF ROPE IN METERS ?.001
WHAT IS SPECIFIC GRAVITY OF ROPE ?1.5
WHAT IS INTEGRATION STEP SIZE IN METERS ?.05
WHAT IS THE ANGLE AT THE GROUND IN DEGREES ?46.6
WHAT IS THE TENSION AT THE GROUND IN KGMS ?4.75
WHAT IS WIND IN METERS PER SECOND ?9.7

THE ALTITUDE IS 435.312 METERS
THE LINE OF SIGHT ANGLE IS 61.9494 DEGREES

WHAT IS WIND IN METERS PER SECOND ?10

THE ALTITUDE IS 438.367 METERS
THE LINE OF SIGHT ANGLE IS 62.9298 DEGREES

WHAT IS WIND IN METERS PER SECOND ?10.3

THE ALTITUDE IS 441.352 METERS
THE LINE OF SIGHT ANGLE IS 63.9568 DEGREES

Fig. 12 — Sample interactive computer run used in finding the windspeed from surface measurements on the tether line

SHIPBOARD KYTOON OPERATION

A tethered kite balloon flying from a ship does have hazards which must be kept in mind by the operator.

Downwind from the ship is a region where both the wind velocity and pressure fields are disturbed by the presence of the ship. The region of disturbed flow is here defined as the region in which the velocity field is disturbed by 5% or more from the background flow. The disturbed region can be divided into three principal characteristic zones illustrated in Fig. 13. The displacement zone is relatively free of large-scale turbulent eddies and hence has no adverse effect on tethered vehicles. Some information on the flow characteristics within the wake boundary can be obtained by considering the experiments of Fail, Lawford, and Eyre [3], in which flat plates were suspended normal to the wind in a low-turbulence wind tunnel.

These results were summarized by Halitsky [4] for the case of a square plate of side p . The range of applicability of these results is $0.5 < x/p < 5$ for a mean uniform stream velocity. The wake axis is coincident with the x axis and the origin is at the center of the plate.

1. The wake boundary originates at the edge of the plate and develops into a paraboloid of revolution. The curve of the boundary in the longitudinal section through the axis may be approximated by

$$y = p(x/p)^{1/4}$$

where y is the radial distance from the axis at the longitudinal distance x .

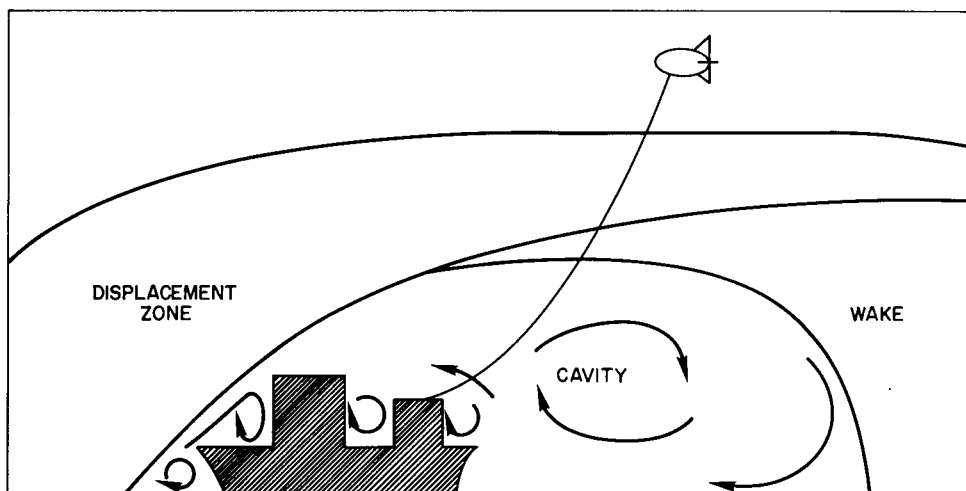


Fig. 13 — The distorted airstream areas about a ship

2. The mean velocity at the center of the cavity is about 60% of the background flow velocity and is opposite in direction.
3. The cavity boundary originates at the edge of the plate but develops into an approximate ellipsoid of revolution of length equal to $2.83 p$ and radius at the midlength equal to p .
4. The longitudinal turbulence intensity, $(v - \bar{v})/\bar{v}$ at $x = 3.6 p$, varies from 0.11 at the axis to 0.22 at $y = 0.8 p$ and falls to substantially zero in the background flow.

As a first-order approximation, these results can be incorporated into the study of launching hazards to tethered balloons. The following two aerodynamic features of the wake and cavity cause dangers to the tethered vehicle. Within the cavity, vortices exist which can have disastrous effects on kites or kite balloons. A kite balloon has been observed caught within the cavity and forced to the sea surface. Outside the cavity but within the wake, unpredictable turbulent eddies may await the kite vehicle. Both of these effects are proportional to the undisturbed wind velocity. Although the geometry of the wake and cavity boundaries appears to remain constant with respect to increases in wind-speed, these wind-related effects put an upper limit on operational windspeeds. Experience has shown that with relative windspeed in excess of 10 m/sec, violent eddies occur, and the probability that the kite balloon will be caught up in one of these before it can rise above their influence is great. On the other hand, the lift provided by the aerodynamic shape of the kite and available for supporting experiments is a rapidly increasing function of relative windspeed. Therefore, there is a "window" in relative windspeeds for a particular load in which safe launches can be made. If the windspeed is less than that required, the loaded kite balloon will not raise the instrument package to the desired height. If the relative windspeed is greater than 10 m/sec, the chance of the kite balloon being caught in a violent eddy or forced into the sea is great. The upper limit of windspeed remains relatively fixed with respect to instrument loading, while the lower limit increases with

instrument loading; thus, increasing the load narrows the operation window. As an example, the launch window experimentally determined for the USNS *Hayes* and a net load of 1.2 kg is between 6 and 10 m/sec.

At this point, it is desirable to have a digital model which will plot the ascent path of a kite balloon in order to determine how best to avoid the cavity and turbulent wake zones. This may be accomplished by the simultaneous integration of Eqs. (10), taking into account the proper boundary conditions. From Eqs. (7) and (8), the lift and drag of the vehicle are known and both the balancing tension and the angle in the tethering line at the vehicle can be calculated, as was done for the simple model. If the integration of Eqs. (10) is started downward with known values of lift and drag and if the origin of the coordinate system is defined at the vehicle, then the values of T , θ , x , y , and s are known at each increment of line below the vehicle if the wind force is known.

If the values of x and y defined above are plotted, they are the focus of the position occupied by the kite balloon during a slow ascent or descent in a coordinate system located at the shipboard winch. The calculated position of the tethered vehicle can be compared with the estimates of the geometry of the wind wake to determine if the rise path of the kite balloon goes through the cavity or wind wake.

Figure 14 shows a plot of such rise paths for a windspeed of 7.5 m/sec and an instrumentation loading of 1.5 kg. Line FG defines the boundary of the ship's wind wake. Tethered vehicles operating below this line are in danger of being caught in a strong down-draft. Line OAC is the path which would be taken during the launch or recovery of an unloaded kite balloon. Line OD is the path taken by a kite balloon with the payload attached to its underbody. The chance of losing both payload and vehicle is very great, using path OD. Consider the following technique where an unloaded vehicle ascends to point A along path OA. At this time, the payload is attached to the tether line at the surface and the whole system is allowed to continue on upward. The kite balloon will now travel along path AB, while the payload will pass along line OE. The advantage of this technique is that the payload is kept safe at the expense of a few meters of maximum obtainable altitude.

Another technique which can be used to increase the chances of a good launch or recovery of a kite balloon system involves adjusting the ship's heading and speed to keep the relative wind within the required window. After the vehicle climbs above the turbulent wake, a higher relative wind can be tolerated, and the ship can continue on its way. This technique allows launching a kite balloon that normally could not be launched under the ship's normal course and speed.

In Part I of this report, the stress was on predicting the maximum altitude which could be obtained by a particular tethered vehicle. When the wind loading on the tether line was neglected, this simple analysis gave the unrealistic result of an unlimited altitude ceiling, given enough wind velocity. The more accurate numerical analysis in Part II may also be applied to predict the maximum altitudes which can be obtained with a particular vehicle, instrument load, and windspeed. The numerical integration referred to earlier is continued until the value of θ at the ground passes through zero. At this point, there is a maximum in altitude determined for each value of wind entered into the calculations as a parameter. Figure 15 shows a comparison of the results of the numerical analysis, the

results of the simple analysis of Part I, an adaptation of Kochin's [2] analytical solution, and some experimental points obtained with a kite balloon equipped with an altimeter and operated from the USNS *Hayes* during February 1974. The theoretical solutions have input parameters that correspond to the experimental values as closely as possible. Kochin's analytical solution has the built-in assumption that the angle θ at the kite balloon is $\pi/2$. This is tantamount to saying that there is zero wind drag on the tethered vehicle. Therefore as one would expect, the numerical analysis corresponds reasonably well with the Part I solution for low lift-to-drag ratios and low winds. If, however, the lift-to-drag ratio is high, the numerical solution corresponds with the Kochin theory.

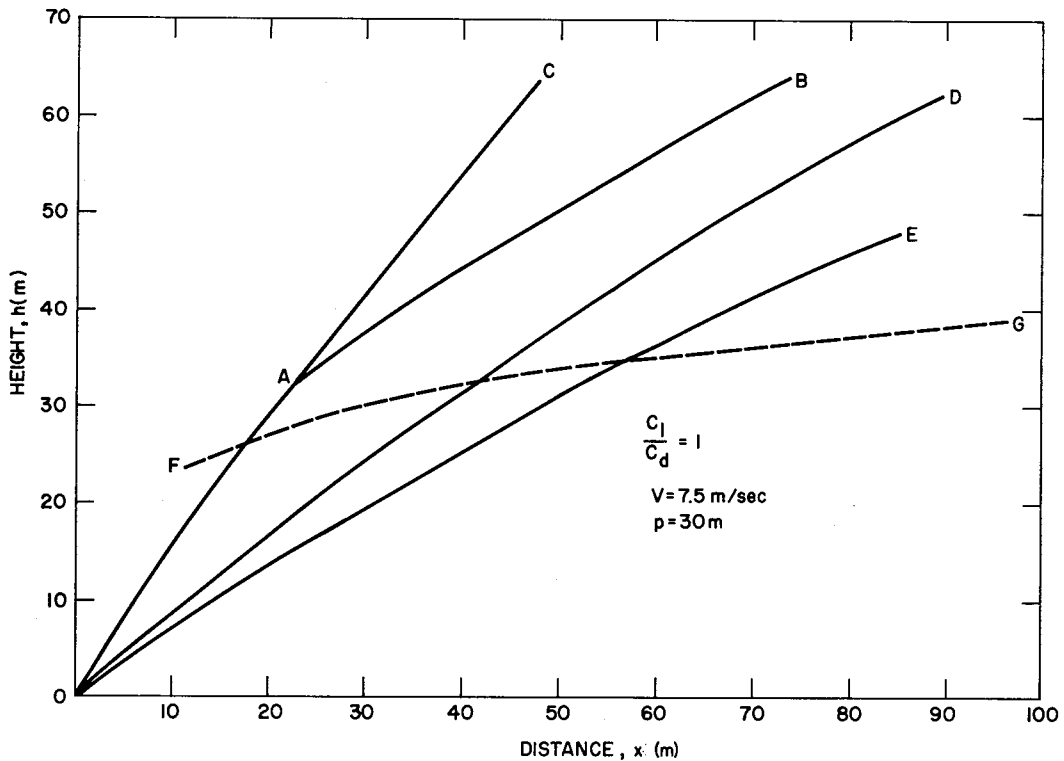


Fig. 14 — Plots of predicted flight paths with respect to the turbulent wake of a ship represented by the area below line FG. See text for details.

Although the experimental points contain considerable scatter, it appears that they do indicate that the lift-to-drag ratio is between 1 and 10 for the kite balloon. On the other hand, a spherical tethered balloon has a low lift-to-drag ratio and the analysis of Part I is applicable here for low wind conditions.

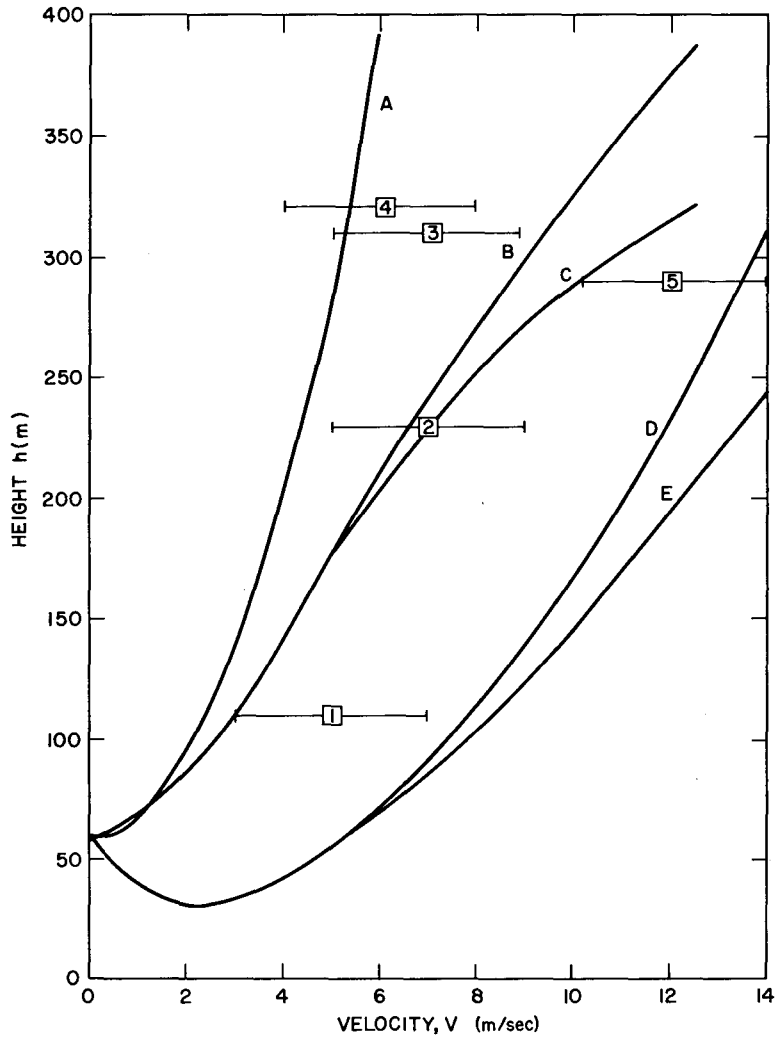


Fig. 15 — Maximum altitude predictions for various methods described in text. Squares represent maximum altitudes obtained at sea with a small kite balloon system. Curve A is from Eq. (9) with $C_l/C_d = 10$, $I = 9.8$ N and $w = 0.038$ N/m. Curve D is the same as curve A except that $C_l/C = 0.3$. Curve B is result for the digital integration method with the specific gravity of the line being 1.22, the diameter of the line being 0.002 m, and $C_l/C_d = 10$. Curve E is similar to curve B except that $C_l/C_d = 0.3$. Curve C is the result of the Kochin theory with the same physical parameters as used above.

REFERENCES

1. Fr. A. Willers, "Ober die Steighöhe von Drachen," Z. Math. Phys. 57, 158-173 (1909).
2. N.E. Kochin, "On the Bending of the Cable of a Kite Balloon under the Action of the Wind," Inst. Mekh. Akad. Nauk SSSR. Prikl. Mat. Mekh. X, 153-164 (1946),
NRL Translation 402.
3. R. Fail, J.A. Lawford, and R.C.W. Eyre, "Low-speed Experiments on the Wake Characteristics of Flat Plates Normal to an Air Stream," Aeronautical Research Council Reports and Memoranda, No. 3120, Aeronautical Research Council, Great Britain (1957).
4. J. Halitsky, "Meteorology and Atomic Energy 1968," D.H. Slade, Editor, U.S. Atomic Energy Commission, TID-23190, 1968, p. 221-232.

Appendix A

PROGRAM TO DETERMINE ALTITUDE AND LINE OF SIGHT ANGLE OF A TETHERED VEHICLE

```
10 PRINT"WHAT IS LENGTH OF ROPE IN METERS";
20 INPUT L
30 PRINT"WHAT IS DIAMETER OF ROPE IN METERS";
40 INPUT D
50 PRINT"WHAT IS SPECIFIC GRAVITY OF ROPE";
60 INPUT S7
70 REM S5 IS UNIT STEP OF INTEGRATING PARAMETER IN METERS
80 PRINT"WHAT IS INTEGRATION STEP SIZE IN METERS";
90 INPUT S5
100 REM ANGLES ARE LABELED A AND TENSION T
110 REM SUBSCRIPTS OF 9 REFER TO VALUES AT THE SURFACE
120 PRINT"WHAT IS THE ANGLE AT THE GROUND IN DEGREES";
130 INPUT A9
140 A9=3.14159*A9/180
150 PRINT"WHAT IS THE TENSION AT THE GROUND IN KGMS";
160 INPUT T9
170 PRINT "WHAT IS WIND IN METERS PER SECOND";
180 INPUT V
190 IF V<0 THEN 460
200 REM G IS THE UNIT WEIGHT IN KGS OF THE LINE USED
210 REM F IS FORCE OF WIND IN KGMS ON UNIT LENGTH OF LINE.
220 LET F=0.0715*V*V*D
230 G=S7*785.39*D*D
240 A=A9
250 X=0
260 Y=0
270 T=T9
280 FOR S=0 TO L STEP S5
290 T1=S5*G*SIN(A)
300 A1=S5*(G*COS(A)+F*SIN(A)*SIN(A))/T
310 X1=S5*SIN(A)
320 Y1=S5*COS(A)
330 T=T+T1
340 A=A+A1
350 X=X+X1
360 Y=Y+Y1
370 NEXT S
380 PRINT
390 PRINT"THE ALTITUDE IS";X;"METERS"
400 A=ATN(X/Y)
410 A3=A*180/3.1415
420 PRINT"THE LINE OF SIGHT ANGLE IS";A3;"DEGREES"
430 PRINT
440 PRINT
450 GO TO 170
460 END
```